Extracting quantitative data from tuft flow visualizations on utility scale wind turbines

S Vey[1], H M Lang[1], C N Nayeri[1], C O Paschereit[1] and G Pechlivanoglou[2]

[1] Institut f¨ur Str¨omungsmechanik und Technische Akustik, TU Berlin,
[2] Germany Technical Director, SMART BLADE GmbH, Berlin, Germany

E-mail: stefan.vey@tu-berlin.de, g.pechli@smart-blade.com

Abstract. First results of a novel measurement technique that allows to extract quantitative data from tuft flow visualizations on real-world wind turbine blades are presented. The instantaneous flow structure is analyzed by tracking individual flow indicators in each of the snapshot images. The obtained per-tuft statistics are correlated with logged turbine data to provide an insight into the surface flow structure under the influence of wind speed. A histogram filter is used to identify two flow states: a separated flow state that occurs at higher wind speeds and a maximal attached flow state that mainly occurs in the lower wind speed range.

1. Introduction

The flow around wind turbine blades can be separated into a time mean velocity component $\overline{U}$ and a fluctuating velocity component u'. Where the instantaneous velocity is $U = \overline{U} + u'$. The time mean velocity component is well defined and in fact the source of power production, whereas the fluctuating velocity component is the source of load variations. These cause fatigue in the structural components of the wind turbine and set a limit to the turbines lifetime. The resulting dynamic stresses, say in the blade root region, can be measured by means of strain gauges. However, the source of these stresses lies in the flow structure on the blades surface.
Numerous methods can be used to asses the flow around a turbine blade (or an aircraft wing): surface pressure measurements as performed in the NREL NASA Ames test [1], stall flags that indicate reversed flow regions [2], oil and tuft flow visualization [3], and other measurement techniques [4]. Some of the above-mentioned techniques require modifications to the internal blade structure or complicated and fragile instrumentation. On the other hand, traditional techniques such as a tuft flow visualization provide instant insight into the blade aerodynamics at a reduced complexity.
In terms of simplicity and spatial coverage the oil flow visualization technique is comparable to a tuft flow visualization. Both methods have their advantages and disadvantages. With the oil flow visualization technique, one can obtain a high spatial resolution also providing insight into the state of the boundary layer. On the downside, it is a one shot method that averages the flow pattern over several rotor rotations including changes in inflow conditions. If several operating points e.g. inflow wind speed, pitch setting, etc. are to be investigated, the blade has to be cleaned and the oil-solution re-applied. This technique is therefore better suited for laboratory flows with defined inflow conditions and eased access to the object under investigation.

Flow indicators, or more specifically flow tufts, have the advantage that they indicate the instantaneous surface flow pattern. Changes in the operating conditions are thus directly reflected in the tuft pattern. Flow tufts have been used for decades both in wind tunnel and free flight experiments. They have also been applied to wind turbine blades [5]. Historically, the tuft pattern was captured by film-photography, later by video-recording. Data evaluation was either performed qualitatively or manually in a tedious way. Advanced techniques used long-term exposures or image overlays to obtain an impression of the tuft-activity (e.g. turbulence level).
The *Institut für Strömungsmechanik und Technische Akustik* at TU Berlin together with SMART BLADE GmbH is currently developing an analysis method that allows to extract quantitative data from tuft flow visualizations. The SMARTviz-technique combines the traditional tuft flow visualization with digital image capturing and processing methods. Per-tuft statistics are obtained that give a deeper insight into the surface flow structures than would be possible with the traditional tuft flow visualization techniques. In addition to the capturing of the tuft pattern the turbine operating parameters e.g. wind-speed, rpm, pitch, yaw, etc. are acquired and related to each image snapshot. The purpose of the project is to study the aerodynamics of real world (i.e. in-the-field) wind turbine blades, dynamic stall effects, and yawed inflow conditions. At TU Berlin the SMARTviz technique is also used for studying the flow patterns around 2D wings [6], generic car models [7], and on the blades of a 3 m diameter research wind turbine. The flow visualization technique is under constant development and current projects deal with the identification of periodic, coherent structures and flow dynamics through tuft flow visualization. Furthermore, the relation between the angular standard deviation of tuft angles and the turbulence intensity is studied in more detail. This relation is not trivial, since the flow tufts do not indicate the velocity itself, but only the flow direction. Additionally the dynamics of the tuft itself are assumed to play a major role.
The purpose of this paper is to give an introduction to the possibilities of this measurement technique.

2. Experimental setup

This tuft flow visualization was performed on a ≈90 m diameter wind turbine in the 2 MW power range. The inflow was unobstructed e.g. no buildings, upstream turbines, etc.. The measurements were performed within two days, including the installation of the flow indicators by a rope-access team. Turbine active power, pitch angle, yaw angle, wind-speed, and temperature were logged in 15 seconds intervals. The image capturing system was synchronized with the wind turbines system clock. Each image snapshot could therefore be related to a certain turbine operating point. All in all, a total of 5000 images were captured by two cameras during the two measurement days. The data presented within this paper was captured on the descending blade at the horizontal blade position. It can therefore be interpreted as a phase average for the horizontal blade position. Each camera captured one image per rotor rotation. The capture frame rate is currently limited by the camera hardware and shooting video results in a lower image resolution. These limitations are hopefully overcome in the future.
Two high resolution DSLRs with 400 mm telephoto lenses are used to perform the SMARTviz. With two cameras two blade positions can be studied in parallel. This is required, for example, to analyze yawed inflow conditions. Here, one camera would capture the ascending blade while the other camera captures the descending blade. Differences in the flow patterns would then reveal yawed inflow conditions.
The cameras can either be operated in manual trigger mode, or by a custom made optical blade passage trigger system that is placed adjacent to the camera. The automatic trigger system can trigger either every passing blade, or every third blade (if only one blade is equipped with flow indicators). A programmable phase delay output is used to trigger the second camera.

Shown in figure 1 is the setup of the camera system in the field. Depending on turbine size and local conditions the cameras are placed 100 to 200 m downstream of the wind turbine.

The blade is equipped with image registration markers and the flow indicator stripes. These

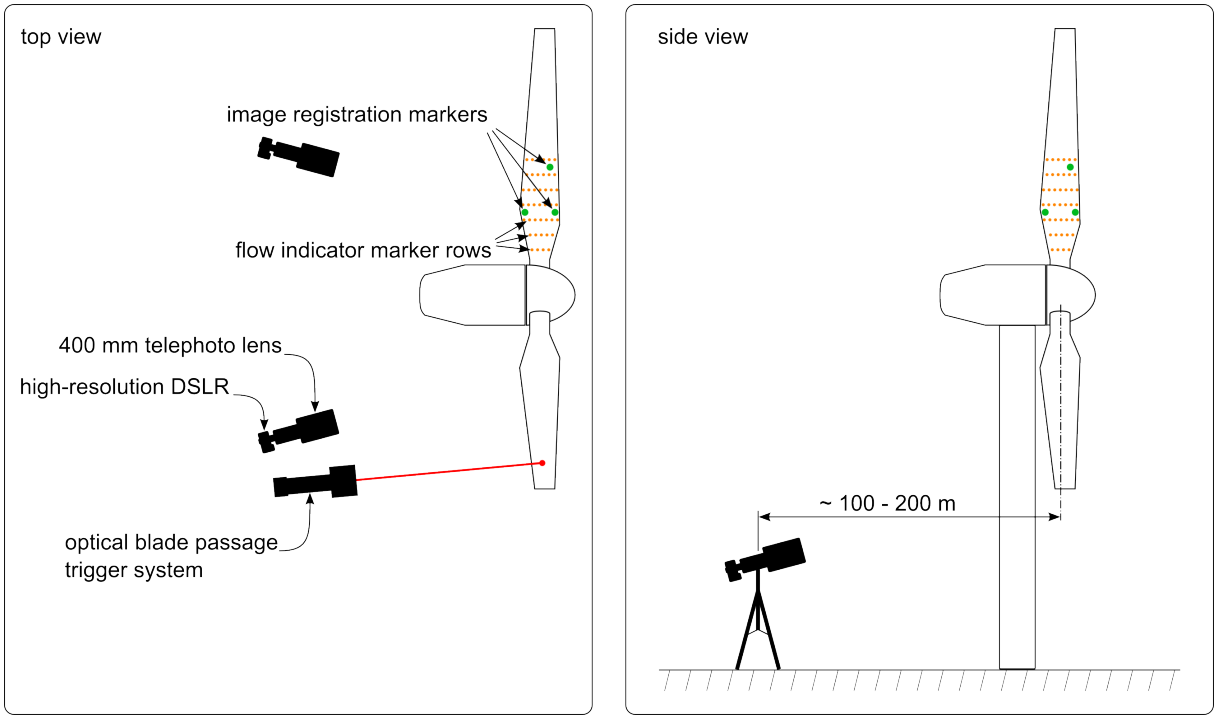

Figure 1. Setup of SMARTviz imaging and trigger system in the field. Usually two cameras are used to capture both the descending and the ascending blade or intermediate blade angles.

consist of a pre-manufactured carrier foil with accurately positioned tuft markers and the flow tufts themselves. The tuft material, size, and color is generally chosen depending on the application. Thinner tufts are used on small wind tunnel models. They are usually white or fluorescent against the black background of the model. For full scale wind turbines a thicker, black, tuft material is chosen. Care has been taken to select a durable tuft material which is still usable after days on the spinning wind turbine and even sustained rain showers.

3. Quantitative tuft flow visualization

Quantitative data is extracted from the raw tuft images by tracking the angular orientation of every tuft in every tuft image snapshot. This data is then used to generate per-tuft statistics from which information about the local flow state can be deduced. The procedure and the methods are discussed in the following.

3.1. Tuft polar histograms

After the raw image data has been processed the mean tuft angles are calculated. These are then interpolated onto an equidistant grid and a line integral convolution (lic) [8] is performed. The resulting image looks similar to an oil flow visualization and shows the surface flow pattern on the rotor-blade. From this flow pattern one can qualitatively determine the cross-flow region, which is shaded pink in figure 2. More in-depth information about the local flow state can be extracted from the single-tuft statistics, or polar histograms (figure 2). The separation location

is determined finding the locations where the chordwise velocity component is zero. This is discussed in more detail in the next chapter.
In the following the single tuft statistics will be discussed. Consider figure 2 where two chordwise tuft rows are discussed in the following. One row is located at the inner part of the blade, near the root (tufts 170 – 180 – 187). It captures separated flow toward the blades leading edge, flow separation at the separation line, and strong cross-flow in the vicinity of the trailing edge. The second row is just outboard of the separated/cross-flow region (tufts 88 – 96 – 103). It clearly shows the increase in the tufts angular standard deviation as the flow travels over the blade from leading edge to trailing edge. For the following discussion the tufts angular standard deviation is assumed to be closely related to the local turbulence level although this relation is not trivial and currently studied in more detail at TU Berlin.
We start our discussion at the row that is located closer to the root. The polar histogram of tuft number 170 is characteristic of an attached flow. The turbulence level is slightly increased because the flow has already traveled a considerable distance from the leading edge stagnation point up to the tuft location.
Tuft number 180 is located on the yellow separation line. Its polar histogram shows an interesting feature: it is bi-modal. This means that there are two stable flow configurations and the flow flips from one configuration to the other. This bi-modality in the angular histogram is discussed in more detail below.
The last tuft on the inner chord-wise tuft row is located within the shaded pink area where strong cross-flows occur. The polar histogram of tuft number 187 reveals a high turbulence level and the 270 deg - orientation is indicative of a strong cross-flow.
The second tuft row to be discussed is located further outboard. Starting the discussion with tuft number 88 shows a typical polar histogram of an attached flow with a low turbulence level. The next tuft (number 96) still indicates an attached flow, only that the turbulence level has somewhat increased. Tuft number 103 is located close to the trailing edge and shows signs of increased turbulence and (normal) flow separation and turbulent cross-flow. Note the, again, bi-modal polar histogram.

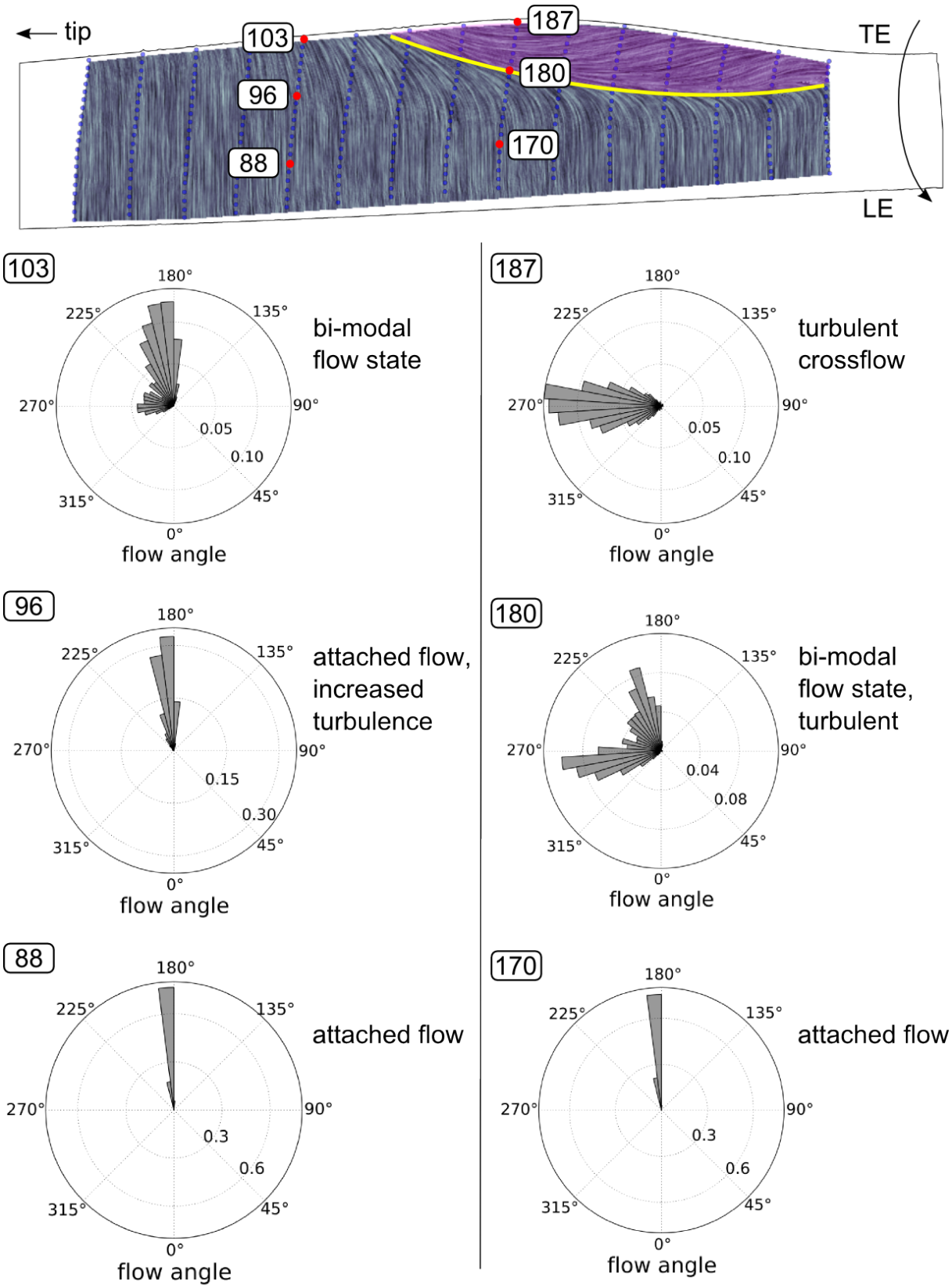

Figure 2. Characteristic polar distributions of tuft angles. Attached flow direction: 180 deg. Separation line (yellow) and cross-flow region (shaded pink) are shown qualitatively here.

3.2. Bi-modal distributions & histogram filter

Prior to focusing on the bi-modal tuft angle distributions and its implications on the mean flow-field the "dumb" mean surface flow pattern is shown together with the tufts angular standard deviation in figure 3. The flow structures are largely similar to what has been discussed above. Note the strong crossflows in the root region and the location of the separation line identified by a zero chord-wise velocity component. As already mentioned above some of the tufts polar histograms showed a bi-modal angular distribution. This is indicative of two stable flow states. In these cases the (circular) mean value of the distribution is no longer a representative value to describe the flow pattern – the mean value rarely occurs. To visualize the spatial distribution of bi-modal flow states a bi-modality coefficient [9] can be defined as:

$$b = \frac{g^2 + 1}{k + \frac{3(n-1)^2}{(n-2)(n-3)}} \tag{1}$$

with the circular skewness g, the circular kurtosis k, and the number of samples n. The higher the value of b the more does the distribution deviate from a normal distribution toward a bi-modal distribution.

The spatial distribution of the bi-modality coefficient is shown in figure 4. Note that increased values of the bi-modality coefficient are concentrated around the separation line with the largest values in the root region. This suggests that the bi-modal flow state is somehow related to a chord-wise variation of the flow separation line. Consider figure 5 where a tuft angle histogram with a pronounced bi-modality is shown. It is interesting to note that the angular difference between the two peaks is approximately 90 deg. The lower distribution has a mean value of 188 deg, which is indicative for attached flow. The higher distribution represents separation/cross-flow. Therefore, at this marker location, the flow jumps between an attached flow state (green shading) and a separated- or cross-flow state (red shading). In order to accurately describe the surface flow field the data-set needs to be filtered for an *maximal attached flow state* and a *separated flow state*. This is done by applying a histogram filter on this individual flow indicator: everything within the green shaded region of flow angles is considered *attached*, everything within

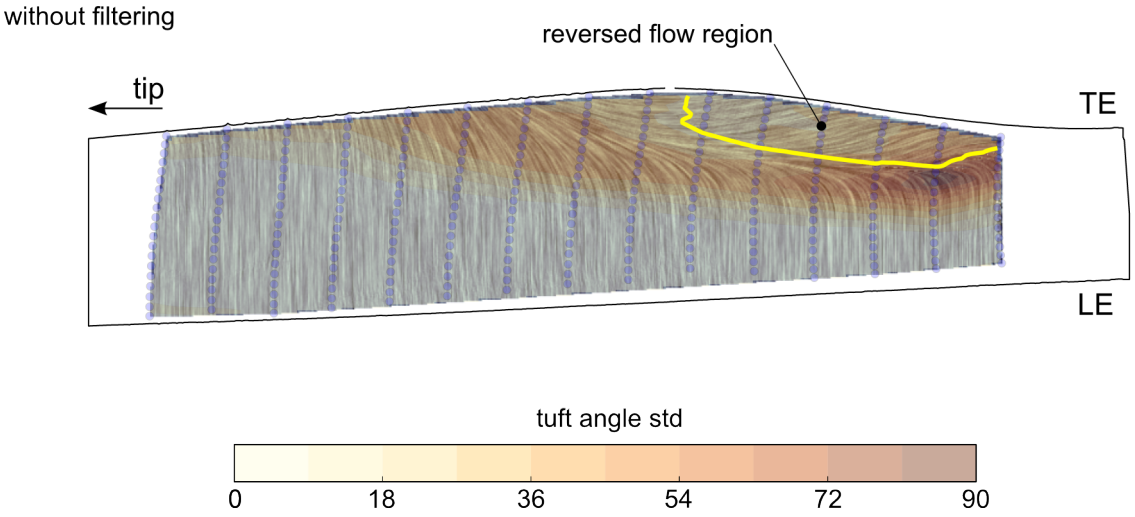

Figure 3. Mean flow pattern shown through LIC-visualization and standard deviation of tuft angle. Flow field in absence of histogram filter. Yellow line denotes the location where the chord-wise velocity component is zero (i.e. separation).

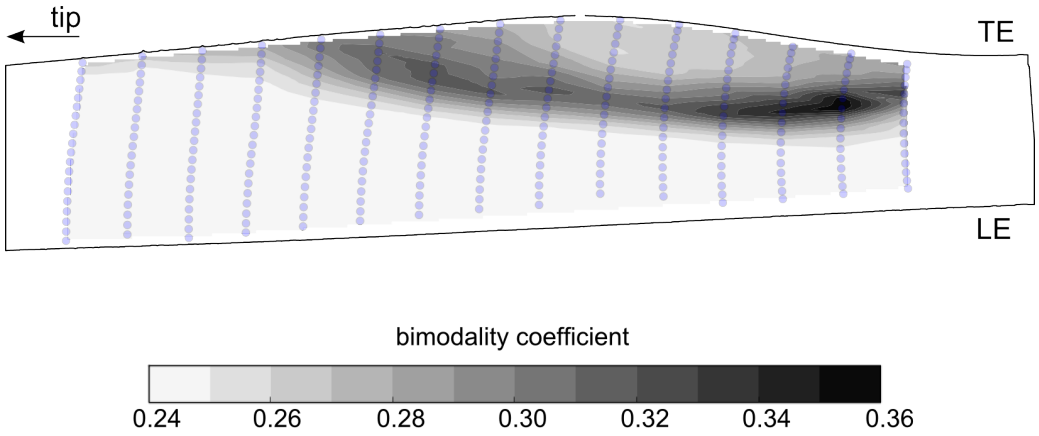

Figure 4. Distribution of the bi-modality coefficient on the blade. Increased levels indicating bi-modal flow state.

the red shading is considered *separated*, and the rest is considered as noise. It is emphasized that for this specific marker, one can indeed distinguish between an *attached* and a *separated* flow state. Whereas when this filter criterion is applied to the complete dataset the flow states are termed *maximal attached flow state* and *separated flow state*, respectively. Applying this filter the two surface flow states (maximal attached & separated) are calculated. Shown in figure 6 is the maximal attached flow state, while figure 7 shows the separated flow state. The red shading is the tufts angular standard deviation, where peak values are reached in the viscinity of the separation location. Note that in the maximal attached flow state the flow separates much further toward the trailing edge (figure 6). The size of the cross-flow region is significantly smaller than in the separated flow state (figure 7). These two flow states represent the extremes on the rotor-blade for the investigated operating conditions. It is assumed that a variation in the separation location is equivalent to a variation of the aerodynamic forces on the rotor-blade, and, consequently, to the structural loads.

One can now ask under which operating conditions is the flow separated and under which operating conditions is the flow maximal attached? Consider figure 8, where the wind speeds are plotted that correspond to the maximal attached and separated states, respectively. The maximal attached flow state is related to the lower wind speeds while the separated flow state occurs mainly at the higher wind speeds. Though it is interesting to note that at the same wind-speed the flow can be maximal attached as well as separated. If the rotor-speed was available one could calculate the tip speed ratio, which might be better suited for a characterization than the wind-speed.

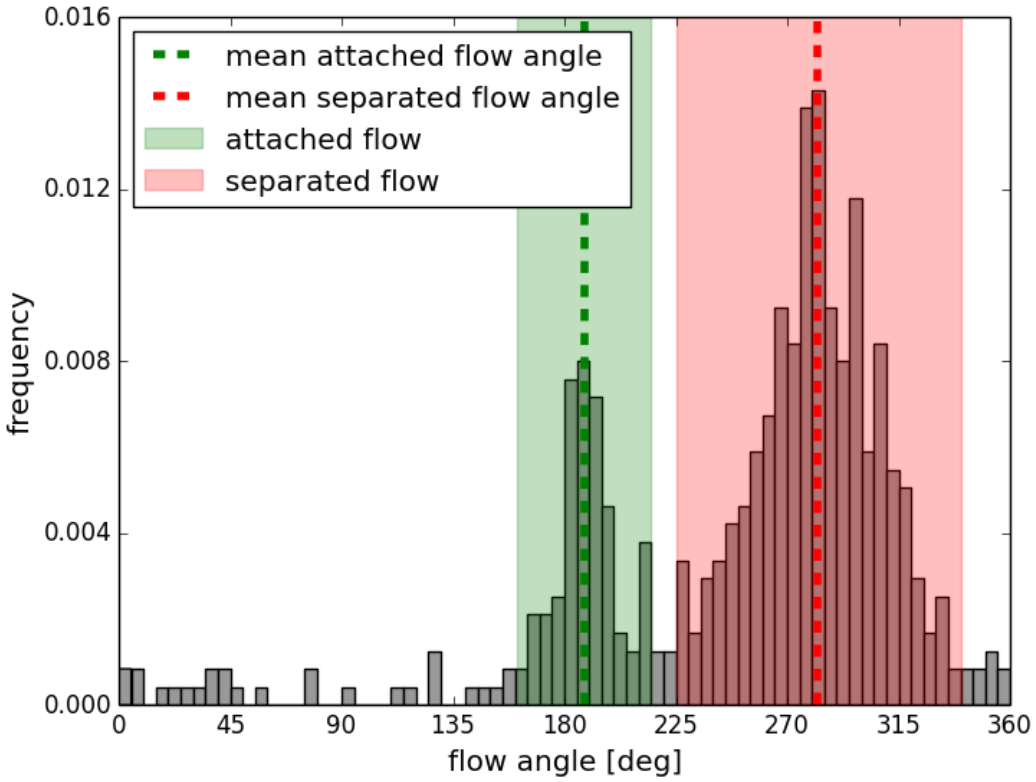

Figure 5. Histogram of tuft showing bi-modal behavior and respective filter settings for *attached* and *separated* flow states. Attached flow direction: 180 deg.

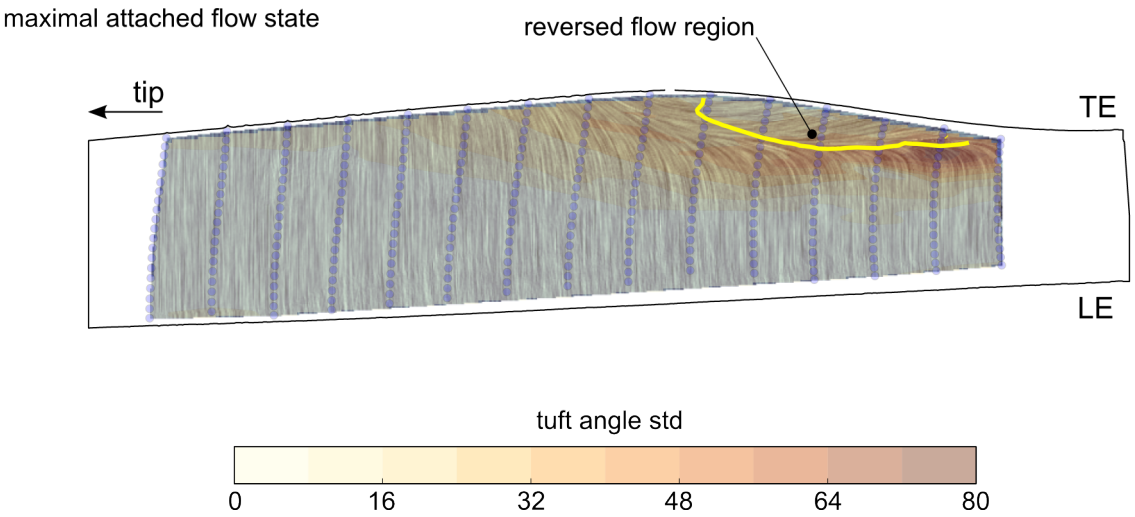

Figure 6. Maximal attached flow-field state. Based on histogram filter for *attached*-region (shaded green) in figure 5. Yellow line denotes the location where the chord-wise velocity component is zero (i.e. separation). Compare to figure 7: note differences in size of cross-flow region and separation location.

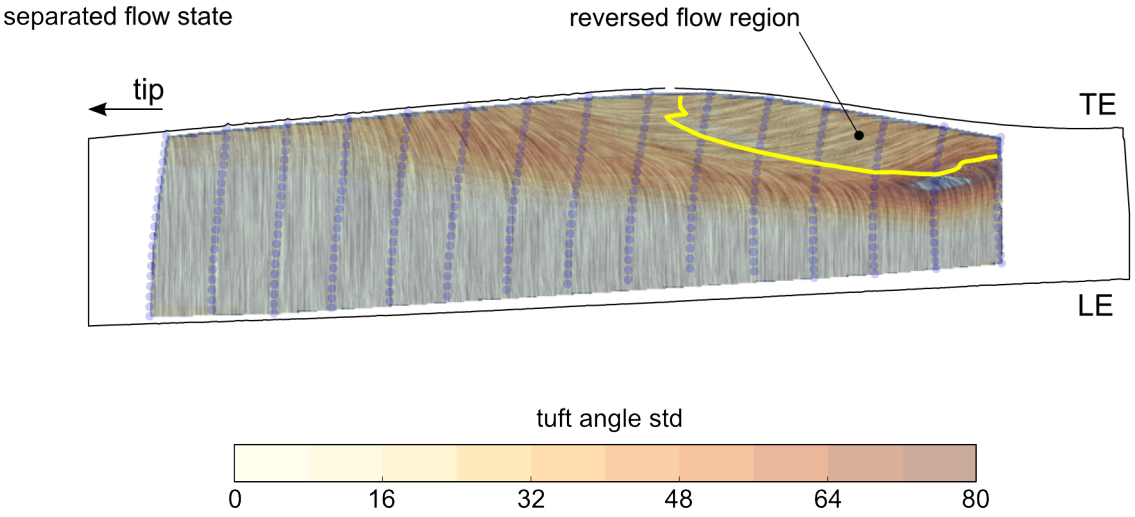

Figure 7. Separated flow-field state. Based on histogram filter for *separated*-region (shaded red) in figure 5. Yellow line denotes the location where the chord-wise velocity component is zero (i.e. separation).

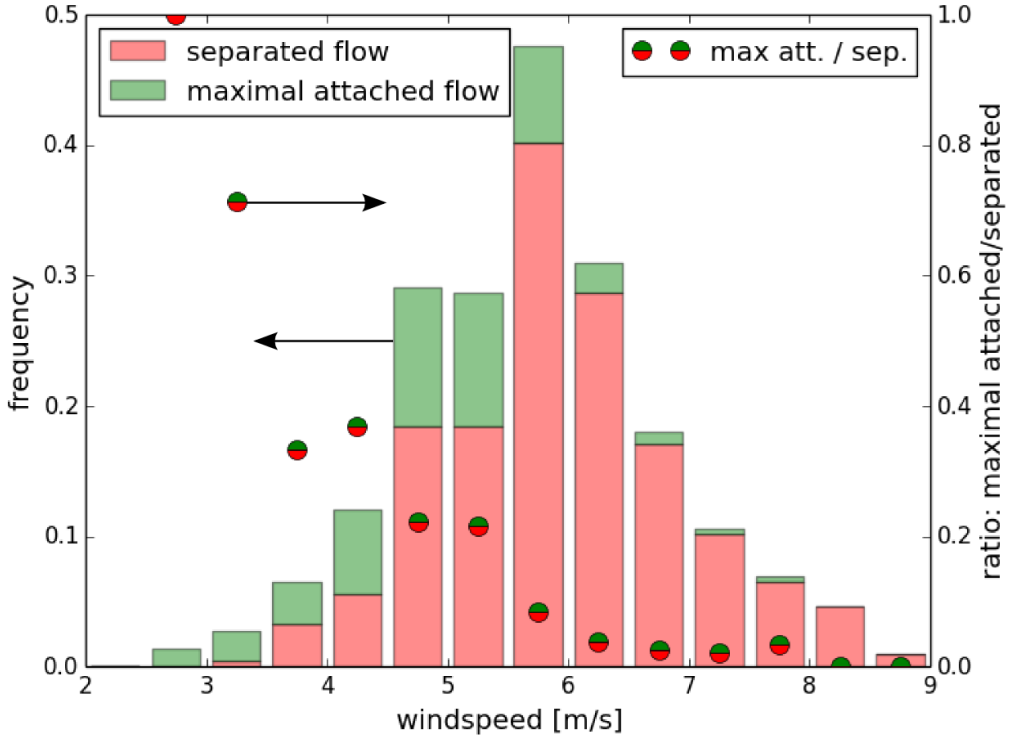

Figure 8. Wind histogram of captured images with maximal attached and separated flow states indicated. For each wind speed bin the maximal attached flow occurences are shaded green while the separated flow occurences are shaded red. The ratio of maximal attached to separated flow occurences is decreasing with increasing wind speed (green-red markers). At 2.75 m/s the flow is in the maximal attached state for all observed occurences (ratio= 1.0). For windpeeds $\leq$ 8.25 m/s solely the separated flow state occurs (ratio= 0.0).

4. Conclusions

First results obtained with a novel flow visualization technique were presented. The technique combines the traditional tuft flow visualization with digital image capturing and processing techniques to extract quantitative data.

Results from a flow visualization on a wind turbine in the 2 MW range were presented and some of the analysis possibilities were shown. The individual-tuft polar histograms were analyzed for bi-modal flow states and two states were identified: a maximal attached flow state and a separated flow state. These flow states represent the two extreme ends of the flow patterns on this specific turbine blade under the inflow conditions of the two measurement days.

In the maximal attached flow state the cross-flow region was found to be considerably smaller than in the separated flow state. Furthermore, the separation line was shifted further toward the trailing edge in the maximal attached flow state. The logged weather data revealed that the maximal attached flow state occurs at the lower wind speeds while the separated flow state is mainly found at higher wind-speeds.

The measurement technique is being actively developed at TU Berlin and SMART BLADE GmbH. In the future this technique could be used to investigate dynamic stall effects and to assess yawed inflow conditions on wind turbines. It can also be applied in other fields such as the aerodynamics of cars, trucks, trains, buildings, wind tunnel tests, etc. to provide a quantitative insight into the flow structures and dynamics.

The low image capture rate of todays very high resolution DSLRs (approximately 4 frames/second) is currently a limiting factor. Higher frame rates can be achieved by using more than one camera. The video recording function of consumer cameras do not deliver the same resolution of a photo and the compression algorithm introduces artifacts to the high frequency video content, i.e. the fast moving tufts, causing the tuft tracking algorithm to fail.

Acknowledgments

The authors would like to acknowledge the support of UpWind Solutions for the installation of the flow tufts and of 3M for providing all the material. SMARTviz was developed at ISTA (HFI) TU Berlin with financial and intellectual support from SMART BLADE GmbH.

References

[1] Simms D, Schreck S, Hand M and Fingersh L J 2001 NREL unsteady Aerodynamics Experiment in the NASA-Ames wind tunnel: a comparison of predictions to measurements NREL/TP-500-29494.
[2] Corten G P 2001 Flow separation on wind turbine blades: Het Loslaten van Stroming over Windturbinebladen dissertation Universiteit Utrecht.
[3] Fisher D F, Del Frate J H and Richwine D M 1990 In-flight flow visualization characteristics of the NASA F-18 high alpha research vehicle at high angles of attack NASA TM-4193.
[4] Nitsche W and Brunn A 2006 Strömungsmesstechnik Springer Verlag ISBN10 3-540-20990-5.
[5] Butterfield C P 1989 Aerodynamic pressure and flow-visualization measurement from a rotating wind turbine blade 8th ASME Wind Energy Symposium TP-3433.
[6] Bach A, Lennie M, Pechlivanoglou G, Nayeri C N and Paschereit C O 2014 Finite micro-tab system for load control on a wind turbine Journal of Physics: Conference Series.
[7] Strangfeld C, Wieser D, Schmidt H-J, Woszidlo R, Nayeri C N and Paschereit C O 2013 Experimental study of baseline flow characteristics for the realistic car model DrivAer SAE 2013 World Congress & Exhibition 2013-01-1251.
[8] Cabral B and Leedom L C 1993 Imaging vector fields using line integral convolution SIGGRAPH '93 Proceedings of the 20th annual conference on Computer graphics and interactive techniques Pages 263-270.
[9] Freeman J B and Dale R 2012 Assessing bimodality to detect the presence of a dual cognitive process Behavior Research Methods Pages 83-97 doi: 10.3758/s13428-012-0225-x.